Superficies y Vacio **8**, 4-12(1999)

Geometrical Structure of the 1/2 ML (2×1) and 1/3 ML (2×3) Ba/Si(001) Interfaces

A. Herrera-Gómez♦
Laboratorio de Investigación en Materiales, CINVESTAV-Qro. A.P. 101, Querétaro, México; and Stanford Synchrotron Research Laboratory, Stanford CA 94305

P. Pianetta
Stanford Synchrotron Research Laboratory, Stanford CA 94305

D. Marshall
Physical Sciences Research Labs, Motorola, 2100 East Elliot Road, Tempe, Arizona 85284

E. Nelson, and W.E. Spicer
Stanford Synchrotron Research Laboratory, Stanford CA 94305

Abstract

The adsorption site of Ba deposited on a clean Si (001) surfaces was measured using X-Ray Standing Wave Spectroscopy (XSW). Two interfaces were considered: half a monolayer (1/2ML) with a (2×1) surface symmetry, and 1/3ML with a (2×3) symmetry. Two (111)-like Bragg reflections, $(\bar{1}\,\bar{1}\,1)$ and $(1\,\bar{1}\,1)$, were utilized in the XSW experiments. From the structural results obtained from these two reflections, and using symmetry arguments, it was possible to establish in three dimensions the coordinates of the adsorption site for the two interfaces considered. In both cases, Ba sits near the center of the square formed by four Si surface atoms, at a height close to the projection of the next ideal Si (001) plane.

PACS numbers: 68.35, 68.55.
Keywords: Ba, Si, XSW, geometry, interface, structure.

I. Introduction

A. The Ba/Si Interface

Barium grows on Si (001) surfaces in a layer by layer fashion even if it is deposited at room temperature, and forms well ordered surfaces when they are annealed to 850-925ºC. Ba makes a good candidate to work as an intermediate layer to grow other materials that can not be grown directly because of their reactivity with Si.

It has been reported[1,2] that, when the deposition is made close to 900ºC, the maximum coverage is 1/2 monolayer (ML). The symmetry of the LEED pattern evolves as the Ba coverage runs from zero to 1/2ML. It starts as (2×1) for the clean surface, changes to (2×3) when the coverage is around 1/3ML, shows (2×6) spots right before the coverage reaches 1/2ML, and end up as (2×1) when the coverage is 1/2ML. A detailed knowledge of the geometrical structure of the (2×1) and (2×3) interfaces is a starting point to the engineering of growing methods for new materials. We studied the geometry of these interfaces using X-Ray Standing Wave Spectroscopy (XSW).

B. Experimental Determination of Atomic Position

XSW has become a clear choice for surface structure studies[3] and also of implanted impurities[4]. XSW allows the determination of the position of surface adatoms with respect to the ideal projection of the substrate crystal. This technique utilizes the x-ray standing wave that is formed when an x-ray impinges on a crystalline substrate at a Bragg condition. This standing wave is due to the interference of the incident beam with the reflected beam, and has exactly the periodicity of the atomic planes of the crystal lattice. If an adatom is located at a position of the unit cell where the electric field of the standing wave is maximum, it will be strongly excited. If the adsorbing site coincides with the valley of the standing wave, the excitation of the adatom will be minimum. It is possible to experimentally measure the strength of the electric field seen by a particular adatom, and with this, to extract its position in the unit cell. For this it is necessary to monitor the yield (Y) from any product of the atom excitation as the standing wave walks through the interplanar distance. Walking the standing wave can be done by sweeping the photon wavelength or the crystal angle through the Bragg

♦ e-mail: alberto@ciateq.mx

condition. In the present study, we measured the position of Ba adatoms by monitoring the photoemission yield from the Ba $3d^{5/2}$ atomic level while the photon energy was swept through the $(\bar{1}\,\bar{1}\,1)$ or $(1\,\bar{1}\,1)$ (see Figure 4) Bragg conditions.

Figure 1 depicts a (rotated) side view of a (001) Si surface covered with Ba. The gray level represent the strength of the electric field of a standing wave generated with the $(\bar{1}\,\bar{1}\,1)$ planes. As it can be appreciated, the magnitude of the electric field seen be the Ba adatoms depends on where is it located with respect to the unit cell. By sweeping the photon energy or angle around the Bragg condition it is possible to sweep the phase of the standing wave throughout the unit cell. In this way, the position of the adatoms can be extracted from the response of the adatom signal as the photon energy or angle is swept around the Bragg condition.

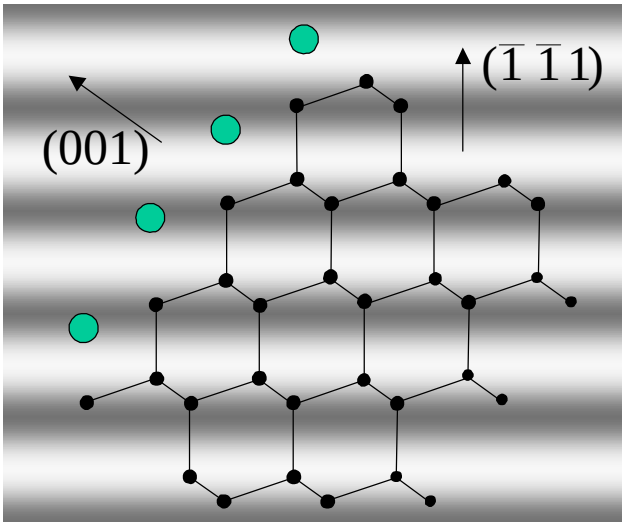

Figure 1. Si (001) surface with Ba adatoms. The gray level indicates the strength of the electric field of the x-ray standing wave. The (111) atomic planes were used to generate the standing wave.

Although in principle three reflections are required to triangulate the position of adsorbed atoms, symmetry arguments can be utilized and, as it will be shown later, only two reflections were required to locate the adsorption site of the surfaces studied.

The excitation rate in the standing wave field of a monochromatic beam of energy E depends on the geometry or position of the adatoms under study through two parameters[5], the coherent distance (D_c) and the coherent fraction (f_c). The D_c can be viewed as an "averaged" perpendicular distance of the adatoms to the atomic planes in units of the interplanar distance, so it assumes values between -0.5 and 0.5 (see Figure 1). The f_c depends on the spread of the positions of the impurities in the interplanar period; its value is maximum (equal to one) when the distribution function is sharp, i.e., when all impurities take equivalent positions (a delta function around one position). The functional form is the following:

$$(1)\quad Y(E) = 1 + \Re(E) + 2 f_c \sqrt{\Re(E)} \cos\left[\eta(E) - 2\pi D_c\right]$$

where η is the phase difference between the incident and reflected beam determining the position of the maximum and minimum of the electric field of the standing wave, and $\Re$ is the intensity of the reflected beam with respect to the incident beam. Both η and $\Re$ are obtained theoretically[5]. As mentioned earlier, the structural information is contained in D_c and f_c.

Because the actual incoming x-ray beam is not monochromatic, Eq. (1) has to be convoluted with the shape of the beam. The shape of the beam can be extracted[7] from a XSW spectra with a known D_c and f_c, or from the shape of the reflectivity. In this work, a gaussian shape was assumed for the incident beam.

II. Experimental Details

A. Sample Preparation

The samples were one inch square Si (001) wafers. The cleaning procedure employed was the following:

- The SiO_2 layer was removed by dipping the sample in $HF:H_2O$ 1:100 for 2 min. A cleaner oxide layer was regrown by dipping it in a $H_2O_2:H_2SO_4$ 1:4 solution for 4 min at 90ºC. It was then water rinsed for 2 min.
- In a nitrogen environment next to the vacuum chamber, the oxide layer was again removed by dipping the sample in $HF:H_2O$ 1:100 for 2 min. This provides an hydrogen-terminated surface. Immediately after dipping, the sample was introduced to the vacuum chamber.
- The sample was annealed to the desired temperature keeping the pressure bellow 5×10^{-9} Pa.

This method provides very clean surfaces. Ba was deposited by evaporating in situ about one monolayer and then annealing to remove excess Ba to the desired coverage. When the Ba coverage is between 1/2ML and 1ML, the surface exhibits a (2×1) LEED pattern, and when the coverage is between 1/3ML and 1/2 ML, it exhibits a (2×3) pattern. To obtain 1/2ML with no excess Ba the samples were annealed at 925ºC for the maximum time (2 min) below which the LEED pattern keeps being (2×1), and above which the LEED pattern starts to show (2×3) spots. The 1/3ML coverage was obtained by annealing at 925ºC for a longer time to obtain 2/3 of the Ba coverage corresponding to 1/2ML. The experiments were performed at base pressures below 3×10^{-10} Pa.

B. Experimental Setup

The position of the impurities was measured with the XSW technique on the 3-3 x-ray beamline of the Stanford

Synchrotron Radiation Laboratory (SSRL). The XSW experiments were performed by sweeping the photon energy, instead of sweeping the angle of the sample, which allowed us to take advantage of the setups of already existing Extended X-Ray Absorption Fine Structure (EXAFS) beam lines at synchrotron sources. Two non-equivalent sets of (111)-type Bragg planes were studied: $(\bar{1}\,\bar{1}\,1)$ and $(1\,\bar{1}\,1)$. The experimental setup including elements of the monochromator, is depicted in Figure 2.

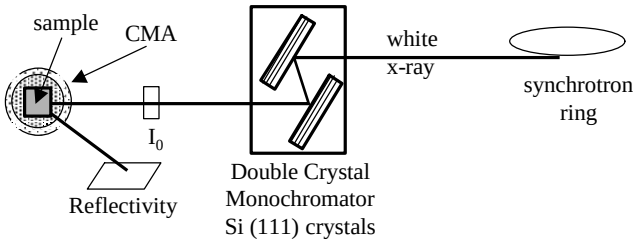

Figure 2. Experimental configuration. The samples were oriented to make the $(\bar{1}\,\bar{1}\,1)$ or the $(1\,\bar{1}\,1)$ crystal planes of the sample parallel to the (111) planes of the monochromator crystals. This optimizes the phase resolution of the standing wave.

The samples were carefully oriented so that the $(\bar{1}\,\bar{1}\,1)$ or the $(1\,\bar{1}\,1)$ planes of the samples were parallel to the (111) planes of the monochromator (see Figure 2 and Figure 3). This configuration, called "non-dispersive", greatly enhances the phase resolution of the standing wave[3]. The experimental procedure to assure proper orientation of the samples is described in Appendix 1. The intensity of the incoming beam was recorded with a grid (I_0 in Figure 2) and the reflectivity was recorded from the total electron yield from a sheet placed in the path of the reflected beam. The CMA recorded the $3d^{5/2}$ Ba signal as the photon energy was swept through the Bragg condition. Figure 3 shows a top view of the sample position.

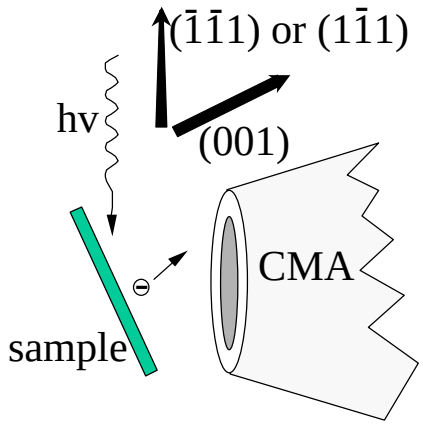

Figure 3. Top view of the sample configuration. The $(\bar{1}\,\bar{1}\,1)$ or the $(1\,\bar{1}\,1)$ crystal vector, both used as Bragg planes, points slightly downwards.

The samples had a slight miscut to encourage 2ML steps in the Si surface to enhance the formation of one domain over the other. The orientation of the crystal and the Bragg vectors considered are shown in Figure 4.

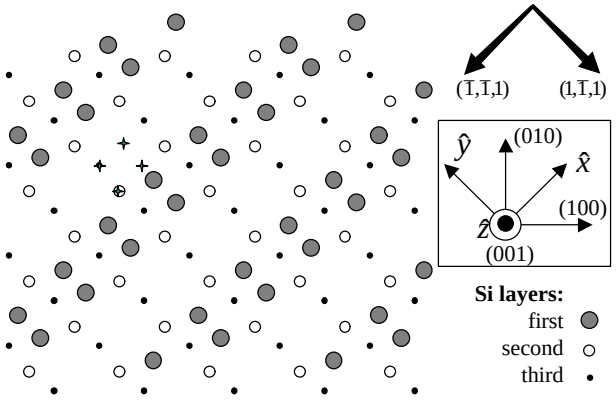

Figure 4. Top view of the Si (001) clean surface. Three layers of Si atoms are represented, the top layer showing buckling. The Bragg planes considered for the study, $(\bar{1}\,\bar{1}\,1)$ and $(1\,\bar{1}\,1)$, are represented with the thick arrows. Notice that these plane vectors point 35.26º up from the surface plane. After one set of data was obtained from one reflection, the other reflection was studied by rotating the sample 90º. The stars represent the high symmetry points of the surface unit cell. The crystallographic vectors and the axis used to calculate the rotations are also shown.

To obtain the strength of the photoemission Ba $3d^{5/2}$ signal, complete photoemission spectra were recorded at each photon energy considered. Because the samples get dirty over time, the level of oxygen was monitored throughout the experiment.

III. Results

Figure 5 shows a typical Ba 3d5/2 photoemission peak. The black line is the best fit and the lower line is the background. Besides the Ba signal (area under the peak), the Si signal was extracted from this data. This was possible because the background is mostly due to inelastic photoelectrons from Si core levels, so the background is proportional to the excitation of Si atoms near (< 200Å deep) the surface.

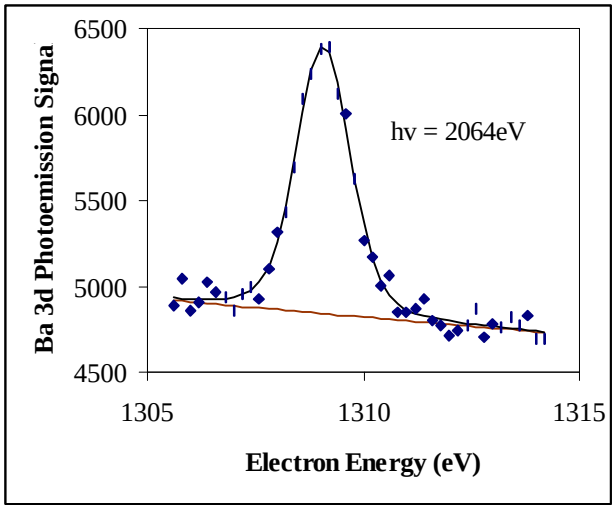

Figure 5. Photoemission signal from Ba $3d^{5/2}$. The Ba signal was extracted from the area under the peak, and the Si signal from the background level at the right extreme.

XSW data were collected for both the 1/2 ML (2×1) and 1/3 ML (2×3) Ba/Si (001) interfaces and for both the $(\bar{1}\,\bar{1}\,1)$ and the $(1\,\bar{1}\,1)$ reflections; they are shown in Figure 6. Each photon energy considered corresponds to a spectrum similar to Figure 5, with the Ba signal corresponding to the area under the curve, and the Si signal to the value of the background at the right extreme.

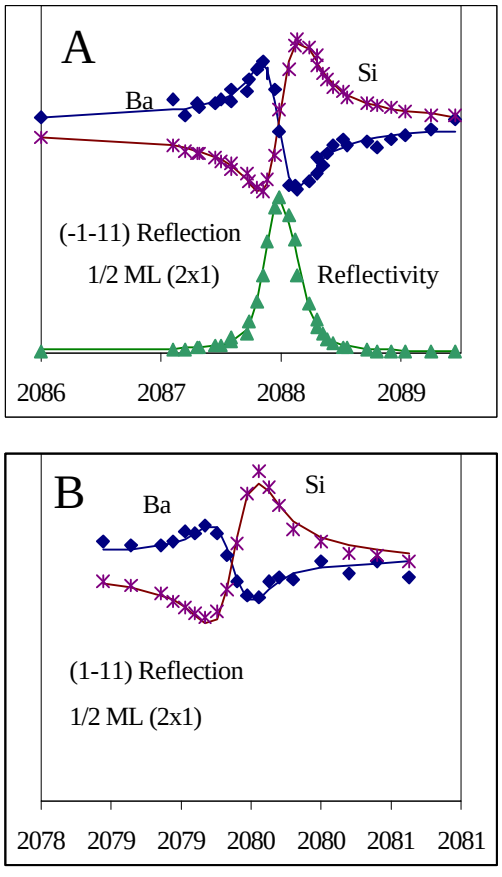

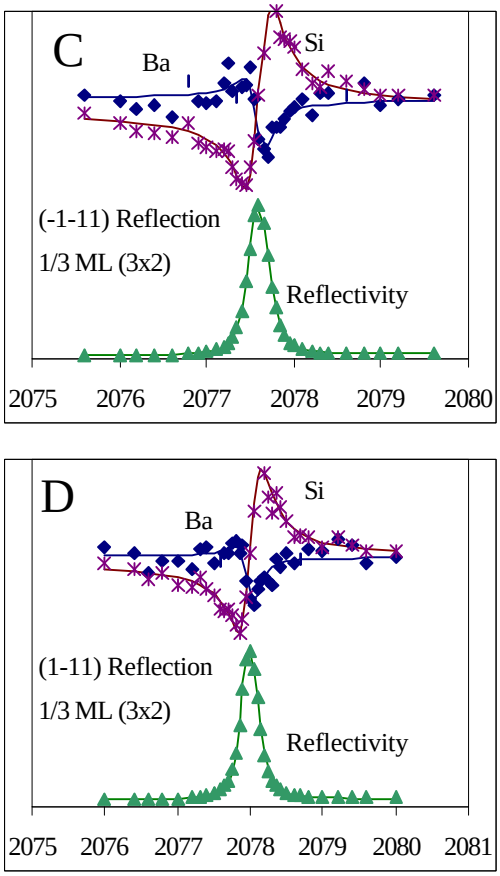

Figure 6. XSW data for both surfaces and both reflections. The x-axis is the photon energy measured in eV.

To perform the fitting of the data, it was necessary to learn about the exact orientation and magnitude of the sample and its miscut. This is because the theoretical prediction of the reflectivity and the standing wave phase (see Eq. (1)) depends on the angles between the surface normal, the incident beam, and the Bragg planes[6]. The miscut was found through the behavior of the Bragg energy with respect to rotations around the surface normal. The procedure is described in Appendix 1. It was found that the magnitude of the miscut was 3.4º± 0.2º. The data was analyzed using a fitting program called XSWfit[7]. The results of the data fitting are shown in Table 1.

Table 1. Structural parameters extracted from fitting the XSW data.

Interface		1/2ML (2×1)		1/3ML (2×3)	
Reflection		$(\bar{1}\,\bar{1}\,1)$	$(1\,\bar{1}\,1)$	$(\bar{1}\,\bar{1}\,1)$	$(1\,\bar{1}\,1)$
Bragg Energy		2087.83	2079.20	2077.43	2077.82
Gauss Width		0.196	0.20	0.167	0.164
Si	D_c	-0.003	0*	-0.005	-0.009
	f_c	0.67	0.61	0.68	0.66
Ba	D_c	-0.3	-0.25	-0.225	-0.205
	f_c	0.63	0.52	0.51	0.51

* The value was assigned to find the coherent distance of Ba.

The results for Si provide a consistency check because the geometry of bulk Si, from which most of the Si signal originates, is known. The values for Si D_c are within 1% of the expected value of zero. The ideal value for f_c at 0 K is $1/\sqrt{2}$ (= 0.7071) because the (111) planes have two non-equivalent atomic positions (see Figure 1). The values for f_c for Si found experimentally indicate a thermal disorder factor, or Debye-Waller factor,[8] close to 0.93.

Although a preferential domain was sought by using miscut samples, the fact that the values for Ba D_c for both reflections are close to each other indicates that there were no strong preference of one domain over the other. If only one domain were present, the difference between the Ba D_c value of one reflection to the other would be equal to 0.25. The appropriate analysis for surfaces with two domains is shown in Appendix 2.

IV. Discussion

The relationship between the structure parameters D_c and f_c to the atomic coordinates is discussed in Appendix 2.

A. The 1/2ML (2×1) Interface

The symmetry and coverage of this interface allows us to make important conclusions about its geometry:

- Because the coverage of this interface is 1/2ML, there is one Ba adatom per every couple of (001) surface unit cells, and because the LEED symmetry is (2×1), every couple of surface unit cells is equivalent to every other unit cell couple.
- From this it can be concluded that all the Ba adatoms assume equivalent positions in every one of the surface unit cell couples.
- We will assume that the adsorption sites should be of high enough symmetry to allow for an extreme (minimum) in the potential energy. This only leaves us[9] with one of the four high symmetry points of the surface unit cell (see Figure 4).

Even though the triangulation was done with only two reflections (see Appendix 2), these symmetry considerations allowed us to locate the Ba adsorption site of this interface in three dimensions. This adsorption site is located in the center of four adjacent Si surface atoms and 1.22Å above the ideal bulk projected Si surface plane. This height corresponds to just 0.13Å below the next ideal bulk projected Si plane. The 2× side view of this adsorption site is represented in Figure 1 and its top view in Figure 7. Although the presence of Ba may unbuckle to some degree the Si surface atoms, Figure 7 depicts the last Si layer with buckles.

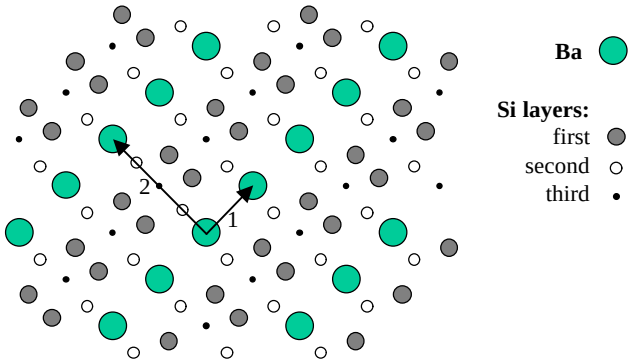

Figure 7. Top view of the Ba adsorption site for the 1/2ML (2×1) interface.

The Ba adatoms can be on top of the dimmers or between the dimmers. The "on top" position can be discarded because the Ba-Si distance would be too short (shorter than the Si-Si distance. Figure 7 depicts the Ba adatoms in the position corresponding to between the dimmers. The difference between the Ba D_c values (-0.3 and –0.25, see Table 1) for the two reflections is due to a preference of one domain (60%) over the other (40%). As mentioned earlier, this preference is due to the sample miscut.

B. The 1/3ML (2×3) Interface

Using the same line of arguments of the last section, it can be concluded that there are two Ba adatoms per every (2×3) surface unit. This allows the possibility of two non-equivalent adsorption sites. The intermediate position of those two sites is very similar but slightly higher to the 1/2ML (2×1) adsorption site: in the center of four Si surface atoms and 1.55Å above the ideal bulk projected Si surface plane (see Appendix 2). The separation of the two sites is 0.24Å, and the preference of one domain over the other was of only 5%. The top view is shown in Figure 8.

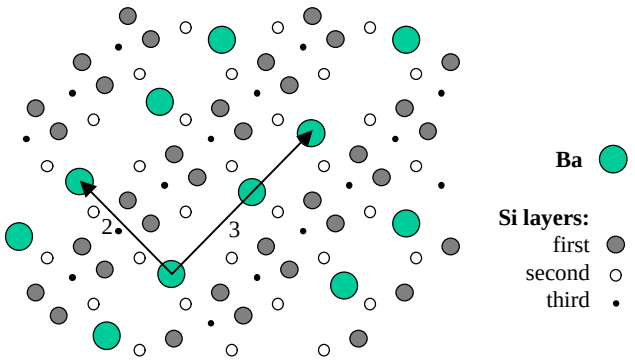

Figure 8. Top view of the 1/3ML (2×3) interface.

The symmetry of the reconstruction allows this separation to be along the vertical direction or along the 3× direction. Because of the large separation between non-adjacent Ba adatoms, their interaction should be negligible, and an extra mirror symmetry along the plane defined by the 3× vector could be claimed. This new symmetry would not allow differences in the z-coordinates of the adsorption sites, leaving only the possibility of a displacement along the 3×

direction. There are still two choices: adjacent Ba adatoms (see Figure 8) may repel or attract each other. We chose to draw them as farther from each other because the Ba grew in a layer fashion on Si (001), which is consistent with the idea that Ba adatoms repeal each other.

V. Conclusions

The geometrical coordinates of the Ba adsorption site of the 1/2ML (2×1) Ba/Si and the 1/3ML (2×3) Ba/Si interfaces were measured using XSW data from two reflections. The 1/2ML (2×1) Ba/Si interface has a unique adsorption site which is located in the center of four surface Si atoms and 1.22Å above them. The 1/3ML (2×3) Ba/Si interface has two adsorption sites whose center is located also in the center of four surface Si atoms, but 1.55Å above them.

Acknowledgments

This work was supported by Phoenix Corporate Research Laboratories-Motorola, by Stanford Synchrotron Research Laboratory, and by CINVESTAV.

Appendix 1: Sample Orientation

In contrast with x-ray difractometers, most vacuum sample manipulators have only two angular degrees of freedom (see Figure 3), so the alignment of the samples requires a special methodology. The first part of this appendix reports the procedure used to align the $(\bar{1}\,\bar{1}\,1)$ or the $(1\,\bar{1}\,1)$ planes of the Si (001) samples parallel to the (111) planes of the monochromator Si (111) crystals. As mentioned in Section 4B, this alignment (non-dispersive configuration) is necessary to optimize phase resolution. The second section outlines the mathematical treatment of the rotations. The last part of this appendix describes the method used to measure the degree of miscut of the samples.

A. Sample Alignment

To optimize phase resolution in XSW experiments it is necessary to align the samples as shown in Figure 9. The Bragg planes of the monochromator crystals are required to be of the same type, (111)-type, as the Bragg planes considered in the sample. In the experiments reported in this paper, all the planes considered are (111)-type.

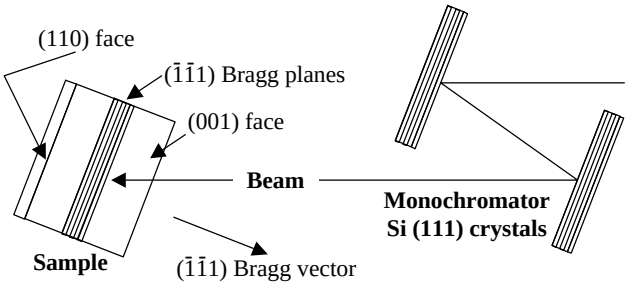

Figure 9. Side view of the Si (001) sample with its (111) Bragg planes parallel to the monochromator (111) planes. This orientation is suitable for XSW experiments.

The incident beam defines a vertical plane, and to achieve the proper sample orientation, the sample Bragg vector is required to lie in that plane and slightly pointing downwards. The orientation of the crystal planes is controlled through the angular degrees of freedom of the sample manipulator: the vertical (q) and the azimuth (f), as described in Figure 10.

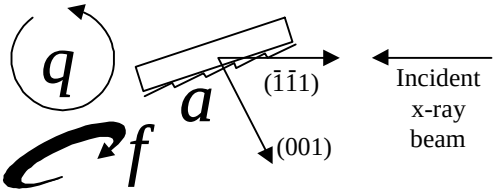

Figure 10. Vertical and azimuth rotations undergone by the sample to reach the non-dispersive configuration illustrated in Figure 9. It also shows a positive miscut a.

This crystal orientation also depends on the miscut a, where a is defined as the angle between the surface normal and the (001) crystallographic vector. The initial position of the sample is defined such that the (001) vector lies in the horizontal plane, and the Bragg vector $(\bar{1}\,\bar{1}\,1)$ is parallel to the incoming beam, as shown in Figure 11.

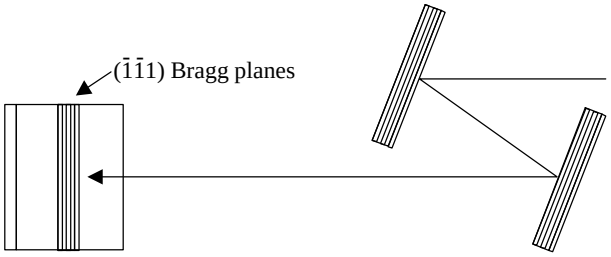

Figure 11. Initial position from where the angles q and f are measured. The Si sample (111) Bragg vector parallel to the incoming beam. After performing the rotations indicated in Figure 10, the orientation described in Figure 9 is reached.

The sample is then rotated by the angles q (~ 2º) and f (~21º). The q rotation removes the $(\bar{1}\,\bar{1}\,1)$ vector from the beam vertical plane. It is then necessary to rotate the sample by an angle f to cause the $(\bar{1}\,\bar{1}\,1)$ vector to lie again in that vertical plane, and in this way reaching the orientation shown in Figure 9. Experimentally it was easy to obtain this

orientation because, for a given positive f rotation (as defined in Figure 10), the Bragg energy has a local minimum with respect to q when the sample Bragg vector lies in the beam vertical plane. This can be visualized by considering that the sample Bragg vector is closer to the incoming beam when it lies in the beam vertical plane, and is taken farther away when q moves in any direction. Figure 12 shows the predicted Bragg energy versus q for f =20º and a miscut of a =3.4º. From this type of behavior it was possible to estimate f .

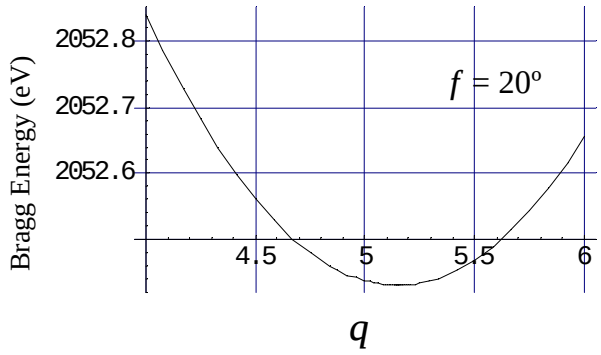

Figure 12. The Bragg energy has a minimum when it lies on the vertical plane defined by the incoming beam.

B. Mathematical Formulas

The reference system employed is shown in Figure 4. Notice that the x-axis is along the dimmers or the (110) crystallographic direction. This system was selected to assure a simple representation of the q rotation matrix. In this system, the matrix representation of the rotations shown in Figure 10 is the following:

$$(2)\qquad T_q = \begin{pmatrix} \cos q & 0 & \sin q \\ 0 & 1 & 0 \\ -\sin q & 0 & \cos q \end{pmatrix},$$

$$T_f = \begin{pmatrix} \cos f & -\sin f & 0 \\ \sin f & \cos f & 0 \\ 0 & 0 & 1 \end{pmatrix}, \quad T_a = \begin{pmatrix} \cos a & 0 & -\sin a \\ 0 & 1 & 0 \\ \sin a & 0 & \cos a \end{pmatrix}.$$

With this transformations, the coordinates of a vector in the lab system (V) and the coordinates of the same vector in the sample system (V'') are related as follows: $V'' = T_a\ T_f\ T_q\ V$. T_q is applied first because its actual rotation axis does not change when T_f and T_a are performed. The first Bragg vector considered is along the $(\bar{1}\,\bar{1}\,1)$ crystallographic direction and its coordinates are $V_1'' = \sqrt{3}/a\left(-\sqrt{2/3}, 0, 1/\sqrt{3}\right)$. The lab system was defined in such a way that the lab coordinates of the incident beam are $\hat{b} = -\left(-\sqrt{2/3}, 0, 1/\sqrt{3}\right)$. Then, as mentioned earlier, the Bragg vector is antiparallel to the incident beam before the rotations are performed. After the sample has been rotated, the coordinates of the beam in the sample system are $-\hat{b}'' = T_a\ T_f\ T_q\ \left(-\hat{b}\right)$, so the Bragg angle b is calculated as follows:

$$(3)\qquad \cos b \equiv -\hat{b}'' \cdot \hat{V}_1'' = \left(T_a\ T_f\ T_q\ \hat{b}''\right) \cdot \hat{b}'' \ .$$

where $\hat{V}_1''$ is the unitary vector along V_1''. The other angles needed for the XSW analysis, the angle between the surface normal $\hat{n} = (001)$ and the incident beam, and between the surface normal and the Bragg vector, can be calculated in a similar way. For the second rotation $\hat{b}$ stays the same, but f is rotated ~ 90º further to get the Bragg vector $V_2'' = \left(0, -\sqrt{2/3}, 1/\sqrt{3}\right)$ in an orientation adequate for XSW experiments. This vector corresponds to the $(1\,\bar{1}\,1)$ crystallographic direction.

C. Calculation of the Miscut

The initial estimate of the sample miscut (provided by the vendor) was $a = 2.5 \pm 1$º. A more precise determination of a was calculated from the behavior of the Bragg energy with respect to the q and f rotations for the (2×1) surface experiments. The orientation of the sample for the first reflection was such that the Bragg energy was 2087.83eV (see Table 1) with the Bragg vector lying on the beam vertical plane. To go to the second reflection it was necessary to rotate q by 3.66º further and f by 91.95º further, and a Bragg energy of 2079.2eV was obtained with the second Bragg vector lying on the beam vertical plane. The only consistent miscut orientation was around the y–axis (consistent with the vendor indication) with a value of 3.4º. The other possibility (miscut around the x-axis) could not reproduce the Bragg energy of the second reflection while at the same time keeping the Bragg vector in the beam vertical plane.

Appendix 2: The Geometric Structure in a Two-Domain Surface

The derivation of the geometrical position of the Ba adatoms from the structural parameters D_c and f_c should take into account that the Si (001) surface is not flat but it has steps of one or more Si monolayers. The (111)-type reflections used for the XSW experiments make no distinction between energetically-equivalent sites located at plateaus differing by an even number of monolayers. But equivalent absorption sites located at plateaus differing by an odd number of monolayers are not equivalent from the XSW perspective.

Figure 13 shows a Ba/Si surface with two (2×1) domains divided by a terrace of one monolayer. The Ba adatoms are drawn in the center of four surface Si atoms. It should be stressed that, just by varying the height of this site, it is possible to sweep all the high-symmetry points shown in Figure 4. Two equivalent origins have been chosen, both at Si third lay sites.[10] The coordinates of the corresponding Ba

adatom (marked with a "×") of the upper domain are $(0,0,(3/4+l)a)$, with l the unknown height above the projected height of the ideal next Si layer (the *xyz* axis defined in the figure was employed). The distance of the upper Ba adatom to its origin along the first Bragg vector in units of the interplanar distance is the following:

$$(4)\quad D_{upper}^{first} = \frac{\sqrt{3}}{a}\left(-\sqrt{\frac{2}{3}},0,\sqrt{\frac{1}{3}}\right)\cdot\left(0,0,\left(\frac{3}{4}+l\right)a\right) = \frac{3}{4}+l\ .$$

The coordinates of the Ba adatom of the lower domain are $\left(0,a/\left(2\sqrt{2}\right),(1/2+l)a\right)$, so its corresponding distance is:

$$(5)\quad D_{lower}^{first} = \frac{\sqrt{3}}{a}\left(-\sqrt{\frac{2}{3}},0,\sqrt{\frac{1}{3}}\right)\cdot\left(0,\frac{a}{2\sqrt{2}},\left(\frac{1}{2}+l\right)a\right) = \frac{1}{2}+l$$

Notice that the difference $D_{upper}^{first} - D_{lower}^{first}$ is always 1/4.

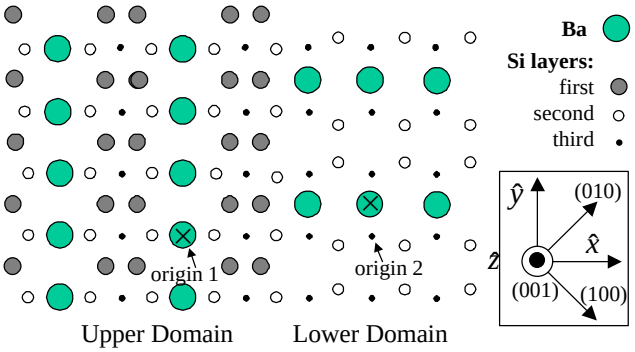

Figure 13. Ba/Si (2×1) surface with two domains. To keep the coherent distances within 0 and 1 (or within –1/2 and 1/2) the position of the Ba adatoms are measured from its local origin[10]. The figure shows the origins used for the first reflection. Origin 1 is hidden below its corresponding Ba adatom, which is marked with an "×". The *xyz* axis system is employed for the analysis. The crystallographic directions are also shown.

As mentioned earlier, the miscut of the sample encourages 2ML steps in the Si surface to enhance the formation of one domain over the other. The distribution function, defined in Reference 4 (see its Equation (2) and above), is then:

$$(6)\quad P(D) = c\,d\left(D - D_{upper}^{first}\right) + (1-c)\,d\left(D - D_{lower}^{first}\right),$$

where c is the fraction of the surface with an upper-type domain. The expression for the coherent distance and coherent fraction are[4]:

$$(7)\quad D_c^{first} = c\ D_{upper}^{first} + (1-c)\ D_{lower}^{first},$$

$$(8)\quad f_c^{first} = s\left|c\ \exp\left(2p\ i\ D_{upper}^{first}\right) + (1-c)\ \exp\left(2p\ i\ D_{lower}^{first}\right)\right|$$

where s is the order parameter or fraction of the impurities at coherent sites[4]. For the second reflection the Bragg vector is $\sqrt{3}/a\left(0,-\sqrt{2/3},\sqrt{1/3}\right)$. It should be notice that the origin was previously defined to calculate the structure factors involved in the XSW analysis[11], and the origins used for the second reflection are not those shown in Figure 13, but are displaced by a vector $\left(0,1/\left(2\sqrt{2}\right),-1/4\right)a$. With this in mind, the corresponding distances for the upper and lower adatoms for the second reflection are:

$$(9)\quad D_{upper}^{second} = \frac{\sqrt{3}}{a}\left(0,-\sqrt{\frac{2}{3}},\sqrt{\frac{1}{3}}\right)\cdot\left\{\left(0,0,\frac{3}{4}+l\right)a-\left(0,\frac{1}{2\sqrt{2}},-\frac{1}{4}\right)a\right\} = \frac{1}{2}+l$$

$$(10)\quad D_{lower}^{second} = \frac{\sqrt{3}}{a}\left(0,-\sqrt{\frac{2}{3}},\sqrt{\frac{1}{3}}\right)\cdot\left\{\left(0,\frac{1}{2\sqrt{2}},\frac{1}{2}+l\right)a-\left(0,\frac{1}{2\sqrt{2}},-\frac{1}{4}\right)a\right\}. = \frac{3}{4}+l$$

The corresponding coherent distance and fraction are obtained from similar expressions to Eqs. (7) and (8). Equation (7) and its similar for the second reflection were employed to calculate the values for l and c reported in Section 4. Notice that, when c is equal to 1/2, both reflections result, as expected, in the same values for D_c and f_c. This would not be the case if the adsorption site were not a high symmetry point, which in turn would yield lower values for the coherent fraction than those found experimentally[9].

References

1 "Process for depositing an oxide eppitaxially onto silicon substrate and structures prepared with the process." R.A. McKee and K.F.J. Walker. U.S. Patent 5,225,031. July 6, 1993.

2 "Adsorption structure of Ba on an Si(001)-2×1) surface." T. Urano, K. Tamiya, K. Ojima, S. Hongo, and T. Kanaji. Surface Science **357-358**, p. 459 (1996). "Ba deposition on Si(199)2×1." D. Vlachos, M. Kamaratos and C. Papageorgopoulos. Solid State Communications **90**, p. 175 (1994).

3 "Surface structure determination with X-ray standing waves." J. Zegenhagen. Surface Science Reports **18**, p. 199 (1993).

4 "Lattice Compression of Si Crystals and Crystallographic Position of As Impurities Measured with X-Ray Standing Wave Spectroscopy." A. Herrera-Gómez, P.M. Rousseau, T. Kendelewicz J.C. Woicik, J. Plummer, and W.E. Spicer. Journal of Applied Physics **85**, p. 1429 (1999).

5 "Dynamical diffraction of x-rays by perfect crystals." B.W Batterman and H. Cole. Reviews of Modern Physics **36**, p. 681

(1964). "A simple x-ray standing wave technique for surface structure determination-theory and application." D.P. Woodruff, D.L. Seymour, C.F. McConville, C.E. Riley, M.D. Crapper, N.P. Prince. Surface Science **195**, p. 237 (1988).

[6] A. Herrera-Gómez. "X-ray standing wave study of the Bi/GaAs and Bi/GaP interfaces." (Ph. D. Dissertation) SLAC-Report-438. Stanford University (1994), and references therein.

[7] XSWfit is a PC program for analysis of XSW data that can extract the shape of the beam usind deconvolution. It is user-friendly and allows to easily define which variables will be optimized. A free fully functional copy can be requested to alberto@ciateq.mx.

[8] R.W. James, "The Optical Principles of the Diffraction of X-Rays," Ox Bow Press, Woodbridge, Connecticut (1947).

[9] Each point (x, y) of the surface unit cell has up to three other energy-equivalent points. Then it is in principle possible to have four different types of patches, each one generating its own (2×1) LEED pattern. Because only the high symmetry points are being considered, and these do not have equivalent points (the equivalent points are themselves), it is only possible one type of patch.

[10] Using the same origin for both Ba adatoms will only add an integer in the coherent distance. This integer is irrelevant, as it can be seen from Eq. (1).

[11] If the same origins are to be used, the calculation for the structure parameters should regard the second reflection as $(\bar{1}\,\bar{1}\,\bar{1})$-type.